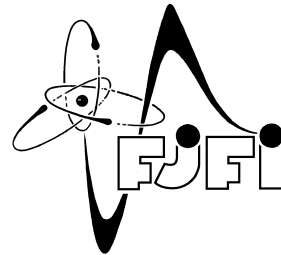
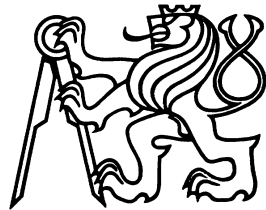


CZECH TECHNICAL UNIVERSITY IN PRAGUE

FACULTY OF NUCLEAR SCIENCES
AND PHYSICAL ENGINEERING

DEPARTMENT OF PHYSICS



**Spectroscopic Investigation
of Laser-Produced Plasma Interaction
with Solid Targets**

BACHELOR THESIS

2009

Michal Šmíd



Katedra: fyziky

Akademický rok: 2008/09

ZADÁNÍ BAKALÁŘSKÉ PRÁCE

Posluchač: Michal Šmíd

Obor: Fyzikální inženýrství

Zaměření: Fyzika a technika termojaderné fúze

Název práce: Spektroskopické studium interakce laserového plazmatu s pevnými terčíky

Název práce: Spectroscopic investigation of laser-produced plasma interaction with solid targets
(anglicky)

Osnova:

- 1) Seznamte se s fyzikálními principy rentgenové diagnostiky horkého hustého plazmatu a spektroskopického studia interakce vysokoparametrového plazmatu s pevnými terčíky.
- 2) Zapojte se do přípravy experimentu na laserovém systému PALS. V rámci této činnosti přispějte k implementaci rentgenových spektrometrů s ohnutými krystaly.
- 3) Sestavte a modifikujte počítačové programy podporující návrh experimentu a zpracování rentgenových spekter.

Pozn. Termín provedení vlastního experimentu vyplyne z aktualizovaného rozvrhu prací na aparatuře PALS. Splnění úkolů bakalářské práce by nicméně mělo být východiskem dlouhodobější spolupráce v navazujícím studiu včetně diplomové práce. Tato činnost bude zaměřena na interakční experimenty s laserově generovaným plazmatem, včetně počítačového vyhodnocení a interpretace získaných experimentálních dat.

Declaration

I hereby declare that this diploma thesis is completely my own work and that I used only the cited sources.

Prohlášení

Prohlašuji, že jsem svou bakalářskou práci vypracoval samostatně a použil jsem pouze podklady (literaturu, projekty, SW atd.) uvedené v příloženém seznamu.

Nemám závažný důvod proti užití tohoto školního díla ve smyslu §60 Zákona č.121/2000 Sb., o právu autorském, o právech souvisejících s právem autorským a o změně některých zákonů (autorský zákon).

V Praze dne _____

_____ podpis

Acknowledgment

I would like to thank to my supervisor Ing. Oldřich Renner DrSc. for giving me this interesting topic and for his valuable explanations and advices, and to all who listened to me talking about this topic.

Název práce: **Spektroskopické studium interakce laserového plazmatu s pevnými terčíky**

Autor: Michal Šmíd

Obor: Fyzika a technika termojaderné fúze

Druh práce: Bakalářská práce

Vedoucí práce: Ing. Oldřich Renner, DrSc., FzÚ, AV ČR

Abstrakt:

Studium interakce plazmatu se stěnami má význam jak pro základní výzkum, tak i pro jeho důležité aplikace v různých fúzních zařízeních. Předkládaná práce přispívá ke studiu této interakce pomocí rentgenových spektroskopických experimentů s dvojfoliovými terčíky. Jsou představeny základní diagnostické nástroje, které byly během těchto experimentů použity, zejména vertikální Johannův spektrometr, poskytující prostorové a vysoké spektrální rozlišení. V závěru je prezentováno předběžné vyhodnocení experimentu pomocí nového programového vybavení vyvinutého v rámci této práce.

Klíčová slova: rentgenová spektroskopie, laserové plazma, interakce plazma - stěna .

Title: **Spectroscopic Investigation of Laser–Produced Plasma Interaction with Solid Targets**

Author: Michal Šmíd

Abstract:

Studying of plasma-wall interaction is of large importance for basic research as well as for its applications in various fusion devices. The basic possibilities of studying this interaction through the x-ray spectroscopic double-foil experiments are introduced in this thesis. Basic diagnostic tools, especially the vertical-geometry Johann spectrometer providing spatial and high-spectral resolution are presented. The trial evaluation using novel codes, developed within the framework of this thesis, is demonstrated.

Key words: Plasma–wall interaction, Laser–produced plasma, x-ray spectroscopy.

Contents

1	Introduction	7
2	Elements of plasma radiation	9
2.1	Line spectrum	9
2.2	Satellite lines	10
3	Double-foil experiments	12
4	Instrumentation	13
4.1	Vertical-geometry Johann spectrometer	13
4.2	X-ray streak camera	17
5	Trial experiment evaluation	20
6	Conclusion	23
A	VJS Analyser manual	I
A.1	Introduction	I
A.2	Image manipulation	III
A.3	Analyzing procedure	IV
A.4	Data export	VII
A.5	Configuration	IX

1 Introduction

The interaction of plasma with solid materials is of large importance for basic research studying the properties and behavior of hot plasmas. It is also important because of its possible applications in future fusion devices.

For example, in tokamaks used in *magnetic confinement fusion*, the plasma diffuses despite the magnetic gradient from the inner parts towards the outer parts of the tokamak. Consequently it reaches its wall and interacts with it. This is one example of the occurrence of plasma-wall interaction, which is intensively studied.

In the most common scheme of indirectly driven *inertial confinement fusion* we can see another example of plasma-wall interaction: The fusion *pellet* is inserted in the hohlraum, the inner surface of which is irradiated with laser beams to produce a plasma which interacts with the pellet.

The *laser-produced plasma* is a plasma generated using an intensive laser beam. The laser beam impinges on a solid target, typically a thin foil, where the matter is ionized and a plasma jet perpendicular to the target is produced. This represents a very efficient tool for investigating the plasma-wall interactions, because the expanding plasma jets can produce different interaction scenarios.

A very efficient diagnostics of such plasmas is based on the x-ray emission spectrometry.

The aim of this thesis is to describe the laser-plasma wall interaction experiments performed in PALS laboratory, which are directed to the acquisition of experimental data necessary for verification of theoretical models of plasma wall interactions and which should contribute to the understanding this phenomena.

The main diagnostic tool in those experiment was the *vertical-geometry Johann spectrometer* (VJS), as described further, which records the high-resolution, spatially resolved spectral data on an x-ray film.

1 Introduction

The processing of the recorded spectra from VJS was the main part of my bachelor work. It consisted of calibrating the scanner and developing a software package for spectra reconstruction.

2 Elements of plasma radiation

The radiation emitted from hot dense plasmas is probably the most important diagnostic tool for these plasmas, because it carries information about the local plasma conditions. For short life-time plasmas, that we focus on in this thesis, the x-ray radiation is a very efficient diagnostic tool.[1]

The emission spectrum is produced by electron transitions, which can be classified with respect to the initial and the final transition states to *free-free*, *free-bound*, and *bound-bound* transitions. It is obvious that the photons emitted during the first two types of processes contribute to the *continuous spectrum*, while the latter process produces photons with discrete energy spectrum and therefore contributes to the *line spectrum*.

2.1 Line spectrum

The *line spectrum* occurs only in plasmas where ions are not fully stripped. In hot dense plasmas, that we are concerned, this is true only for the intermediate and high-Z plasmas.

The main process contributing to the line spectrum is the *spontaneous decay* in which an excited ion decays into a lower, usually ground state, emitting a photon with energy corresponding to the difference between the two electron states. The energies of those lines are given by the Bohr formula,

$$E = \frac{Z^2 e^3}{2a_0} \left(\frac{1}{n_l^2} - \frac{1}{n_u^2} \right), \quad (2.1)$$

2 Elements of plasma radiation

series	abbrev.	n_l
Lyman	Ly	1
Balmer	Ba	2
Paschen	Pa	3
Brackett	Br	4
	...	

Table 2.1: Names of spectroscopic series

where n_l and n_u are the principal quantum numbers of the lower and the upper state of the transition.

For the hydrogen-like ions (that is ions with only one bound electron left), the lines are organized into *series* according to the final state of the transition. The series are denoted by names, as seen in table 2.1. The lines from each series are denoted with a Greek letter in its subscript, e.g. Ly_α refers to $n_l = 1$ and $n_u = 2$.

2.2 Satellite lines

Satellite lines constitute another part of the line spectrum. Usually they appear as low intensity lines near strong *parent* lines. They are caused by the decay of double- or multiply-excited ion.

If one of the excited electrons of a multiply-excited ion decays into a lower state, it emits a photon with energy similar to that emitted from the same transition in a single-excited ion. The presence of another excited electron, so called *spectator*, slightly modifies the electric potential of the ion and thus the energy of the transition levels and the wavelengths of the emitted photon.

This means that for each configuration of states of *spectator* electrons, there is a separate satellite line.

Near the Ly_α transition in hydrogen-like ions, the satellite lines corresponding to different states of the spectator electron are distinguished by the capital letters. In our measure-

2 Elements of plasma radiation

ments we have focused on the J satellite, which is produced with the spectator electron in one of the $2p$ states.

The main diagnostic advantage of satellite lines is their sensitivity to plasma parameters (electron density and temperature) and their small reabsorption compared to the resonance line photons.

Each photon emitted during radiative decay can be reabsorbed by the inverse process, the *resonant photoabsorption*. The rate of this process (the number of photons of given energy absorbed per unit time per unit volume) is proportional to the density of ions in the lower state of the corresponding transition.

This means that a photon emitted due to a decay of single excited ion into its ground state can be easily reabsorbed because the density of ions in the ground state is relatively large. In contrast, the satellite-line photons are almost never reabsorbed because the density of the excited ions, which are necessary for the reabsorption, is rather low.

To sum up, the photons of resonance lines are often reabsorbed and reemitted during the transfer from the plasma center to the detector (thus mostly carrying information about the plasma edge), while the satellite lines carry information directly from the place they have been first emitted.

The multiple-excited ions can originate in several processes. One of them is the *dielectronic recombination*, when a free electron is captured into an ionic excited state and the released energy is transferred to the bound electron, which is then also excited. The other way is the *impact excitation*, which may occur twice or more times in a short time period, thus resulting in the multiple excitation of the ion.

3 Double-foil experiments

Here we describe the basic scheme of the double-foil laser-plasma interaction experiments, which have been implemented as described in the next chapter.

The principle of the experiment consists in laser irradiation of the target placed in a vacuum vessel, and the analysis of the x-ray emission accompanying the laser-matter interaction. The target consists of two thin intermediate-Z foils (usually $0.8 \mu\text{m}$ Al and $2 \mu\text{m}$ Mg) with variable spacing (usually $200 - 500 \mu\text{m}$).

As the laser beam impinges on the target, it produces a plasma on the first irradiated foil. The plasma jet expands perpendicularly to the foil surface at both its sides. With respect to the experiment configuration used, there are two possible scenarios:

1. The plasma jet collides with the relatively cold second foil.
2. The laser beam burns through the first foil and impinges on the second foil before the first-foil plasma reaches it. Consequently, there is already a plasma plume produced on the second foil before arrival of the plasma jet and we observe the collision of those two plasmas.

The occurrence of one of these scenarios depends mainly on the laser-foil geometry, first foil thickness and composition, and on the laser beam parameters.

In some experiments, an auxiliary counter-propagating laser beam can be focused on the second foil from the other side to preheat it and thus to vary the conditions of plasma interaction. The most relevant diagnostics for these experiments is based on an analysis of the emitted x-ray radiation. There can be several types of tools providing temporal, spatial or spectral resolution or its combinations.

4 Instrumentation

In this chapter we describe the instrumentation used in the double-foil experiments performed at the PALS Research Center in Prague [2].

The PALS main laser beam is capable of delivering up to 1 kJ of energy at the fundamental wavelength $1.315 \mu\text{m}$, which can be tripled to 438 nm. The pulse length is 250 - 300 ps.

We used two main diagnostic tools: the VJS provided high-resolution spatially-resolved spectral data, and an x-ray streak camera combined with the slit provided spatially and time -resolved measurements of plasma expansion.

4.1 Vertical-geometry Johann spectrometer

The vertical-geometry Johann spectrometer (VJS) is an x-ray spectrometer based on the principle of vertical dispersion. It provides a high-luminosity, high-resolution, one dimensionally spatially resolved spectral data. Here we will describe the basic principles of VJS, for further reference see [3], [4].

The main element of VJS is a cylindrically bent crystal, which defines a Rowland circle (RC). Neglecting the focusation defects, the Rowland circle scheme (Fig. 4.1) guarantees that any ray going from the point on this circle to the crystal is reflected to another point on the RC, which is symmetrically located along the crystal axis.

This means that if the radiation is emitted from a line source lying on the RC, it is reflected and focused to the corresponding line on the RC, where a detector can be placed. In concrete experiments, neither the source nor the detector are positioned perfectly on the

4 Instrumentation

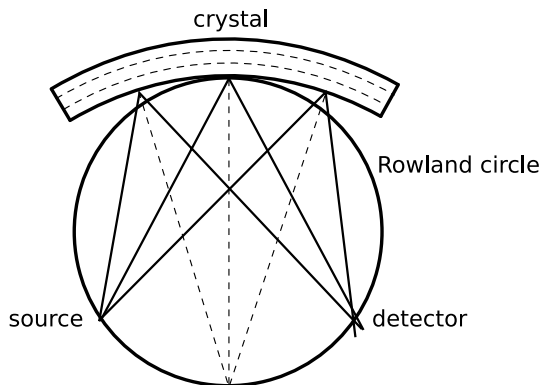


Figure 4.1: Rowland circle scheme.

RC; for elongated sources, both the source and the detector are perpendicular to the central ray connecting the relevant point on the RC with the crystal center.

The dispersion is realized in the vertical direction (i.e. perpendicular to the RC plane). It is based on the Bragg's law, which defines that only photons with the wavelength λ corresponding to the glancing angle θ are reflected, according to the formula

$$\lambda = \frac{2d}{n} \sin \theta, \quad (4.1)$$

where d is the spacing parameter between diffraction planes of the crystal and n is the spectroscopic order.

In our experiment, we used a crystal with the crystal spacing $2d = 0.85084$ nm and the bending radius of $r = 76.6$ mm. The spectroscopic order was $n = 1$. As the detector, x-ray film Kodak CX was used.

The schematic drawing of the VJS setup can be seen in Fig. 4.2. There is a line source on the right side of the image, which emits radiation towards the cylindrically bent crystal in the center of the image. The radiation is reflected towards the detector (on the left), where the film with recorded spectrum is drawn. In the spectrometer there is also a beam stop (not shown in the picture) preventing radiation to go directly from the source to the detector.

Figure 4.3 shows a typical scanned film from VJS with the spectrum recorded. The vertical axis of the image corresponds linearly to the spatial position of the emitted

4 Instrumentation

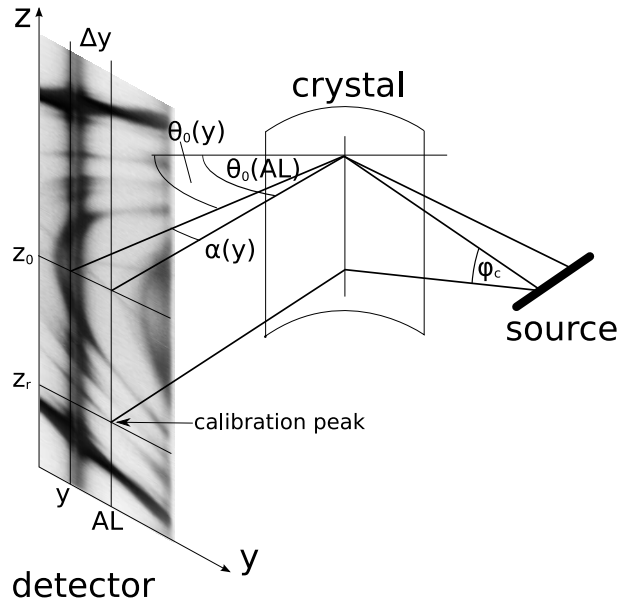


Figure 4.2: Schematic drawing of the VJS setup.

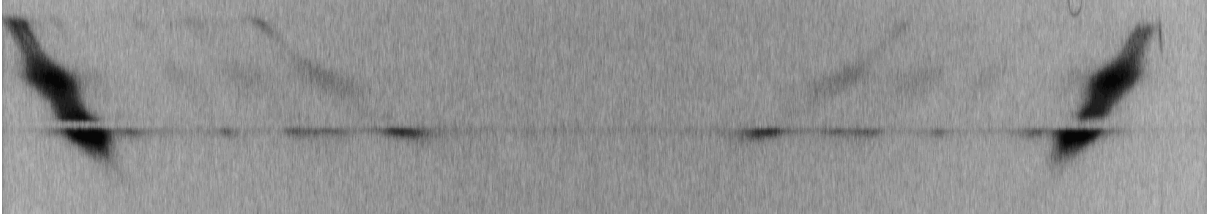


Figure 4.3: Typical scanned film from the VJS with the spectrum recorded.

spectra, the horizontal axis corresponds to the wavelength with a more complicated relation (A.4). The dominant horizontal shape represents a strong radiation emitted from the laser-irradiated foil. The conic-like lines are the spectral lines emitted at different distances from the foil surface. Their special shape is due to the VJS geometry.

4.1.1 VJS spectra reconstruction

The films with spectral records (shown in Fig. 4.3) need to be digitized, calibrated and recalculated to get relevant spectral data.

The digitization can be performed using a precise but not easily available two-dimensional

4 Instrumentation

densitometer. As an alternative to this process we have used a tabletop scanner EPSON PERFECTION V700 with the capability of scanning the films.

First, it was necessary to calibrate the scanner to the optical density, which can later be recalculated to real exposures by using the known characteristic curves of the film.

To get this calibration, we scanned the calibration wedge delivered by the x-ray film producer (Kodak). The measured values stored in the tiff format were fitted with the logarithmic function (because of the logarithmic definition of the optical density). The resulting parameters of this fit were used for the spectra reconstruction. The found dependence of the optical density on the scanned tiff value is seen in Fig. 4.4, where the points denote measured data and the line denotes their logarithmic fit.

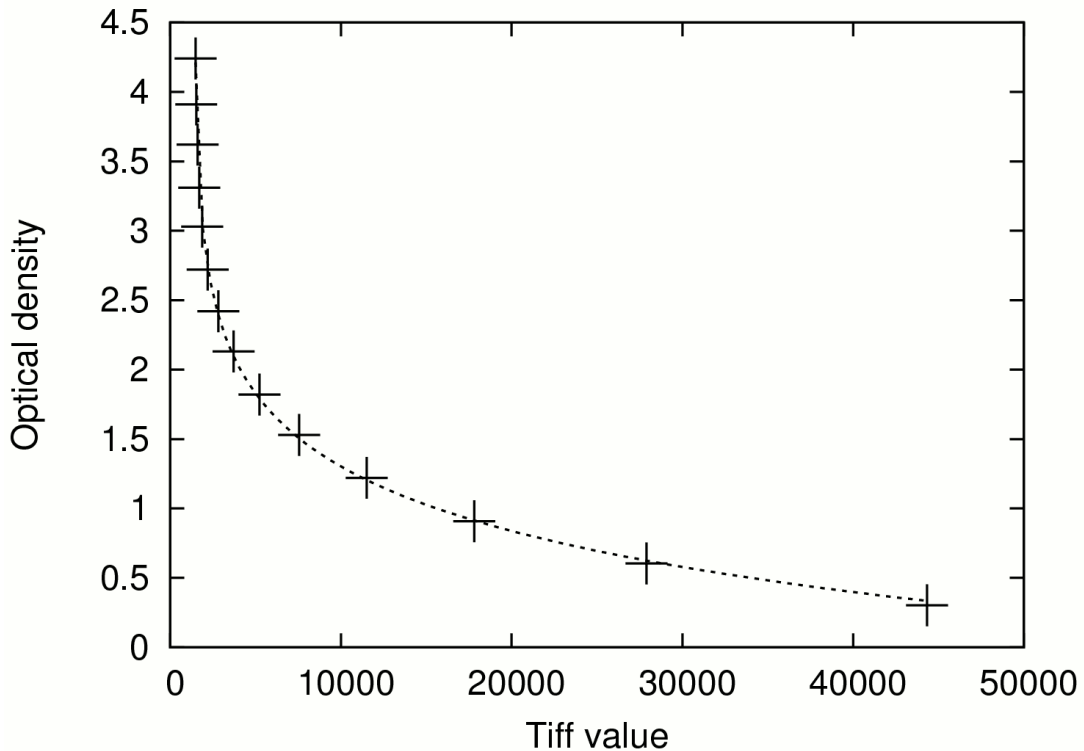


Figure 4.4: Scanner calibration - the relation between the scanned tiff values and the optical density. Points represent the measured values and the line is the fitted calibration function.

For handling the scanned films and the spectra reconstruction we developed a special software package, the *VJS Analyser*, which is described below.

4.1.2 VJS Analyser

VJS Analyser is a software package which was developed for the reconstruction and the analysis of the spectral data from VJS. It is written in the Java language.

Only the main features and capabilities of this application are described here. The details of VJS Analyser can be found in its user manual (appendix A). The illustrative picture of VJS Analyser in its spectra viewing mode can be seen in Fig. 4.5.

The input of this application is the scanned film data file or an equivalent file from densitometer, in format of 16-bit gray-scale TIFF image.

The main functions of VJS Analyser include:

- Viewing and basic manipulation of 16-bit gray-scale TIFF images.
- Precise measurement of the spectral data tilt using correlation algorithm based on the data symmetry.
- Precise determination of the spectral line positions using the least square fit of the appropriate profile.
- Spectra reconstruction - conversion of the raw data into a set of calibrated spectra.
- Viewing and browsing of reconstructed spectra.
- Exporting the selected part of spectral data into a 2D plot suitable for elementary analysis or presentation.
- Exporting the spectral data into tables suitable for further analysis.

4.2 X-ray streak camera

Streak camera is a device providing data with high temporal resolution. It transforms the temporal profile of the measured signal into a 2D spatial profile on a detector. The radiation passing through the entrance slit of the streak camera is converted into electrons and then they are deflected using a strong 1D time-variable electric field. The other dimension is left unchanged, so we get an image with one axis corresponding to time and the other axis corresponding to the spatial distribution of the measured signal.

4 Instrumentation

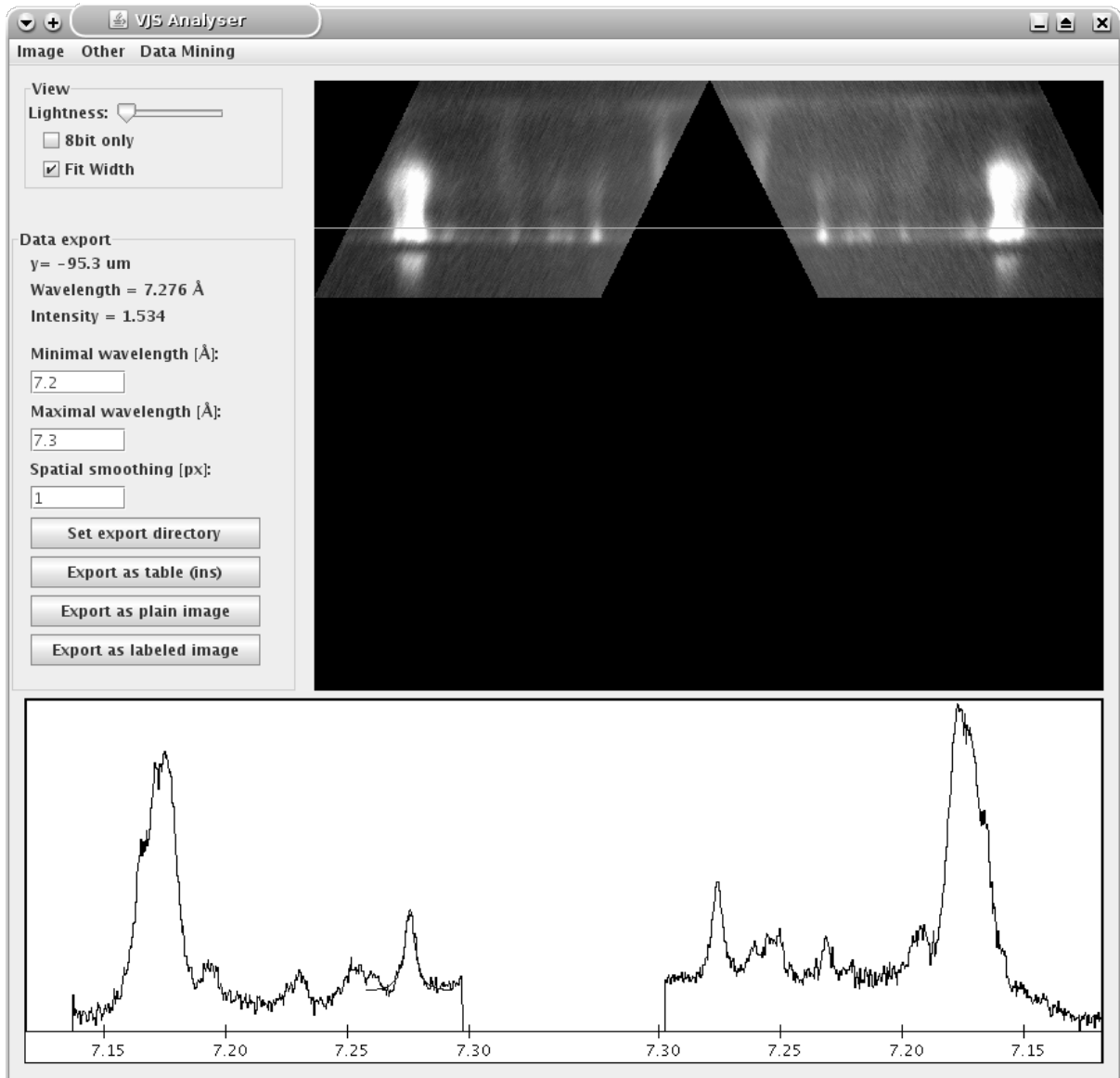


Figure 4.5: Preview of the spectra analysing regime of the VJS Analyser.

4 Instrumentation

We used Kentech low-magnification x-ray streak camera with temporal resolution 2.03 ps/pixel and spatial resolution $2.9 \mu\text{m}/\text{pixel}$. An image from this streak camera can be seen in Fig. 5.3.

5 Trial experiment evaluation

In this chapter we compare two similar double-foil experiments and discuss selected results. The first experiment was performed in 2006 and was described in [5], we performed the second one in January 2009.

Both experiments used double foil targets irradiated from the Al side only. The VJS was set to measure the Al Ly α resonance line with its satellites, especially with the J satellite at 0.72759 nm. Table 5.1 compares the most important experimental parameters. The reconstructed x-ray spectra are shown in Figures 5.1 and 5.2.

	2006	2009
Target material	Al/Mg	Al/Al
Foil spacing	350 μm	450 μm
Laser beam intensity	79 J	112 J
Laser beam frequency	438 nm	1315 nm

Table 5.1: Comparison of the experimental parameters.

In the lower part of Fig. 5.1 (2006 experiment) we can see spectra emitted from the Al foil (positioned at the distance of 0 μm) and those close to the Mg foil viewed on the top (at $\sim 350 \mu\text{m}$). The outer couple of intensive lines corresponds to the resonant Al Ly α line, the less intensive couple in the middle (at $\sim 7.27 \text{ \AA}$) to the J satellite. We can see the emission of the full group of the satellite lines from the Al foil, their disappearance at about 150 μm and their reappearance at the Mg foil. This corresponds well to the record from the streak camera (Fig. 5.3), where the emission from the first foil starts at ~ 0.2 ns, and at ~ 1 ns occurs the interaction of the Al plasma with the plasma generated from the Mg foil.

5 Trial experiment evaluation

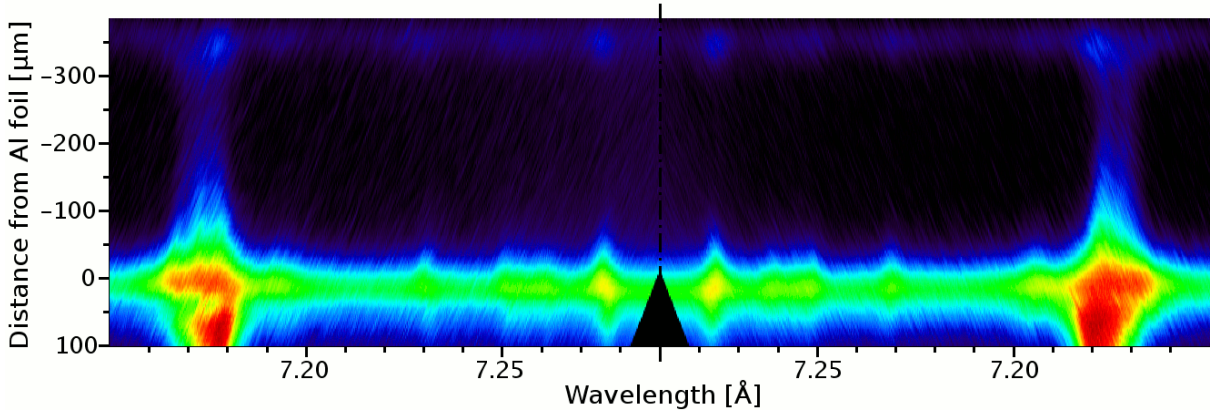


Figure 5.1: Spatially resolved spectra of the 2006 experiment.

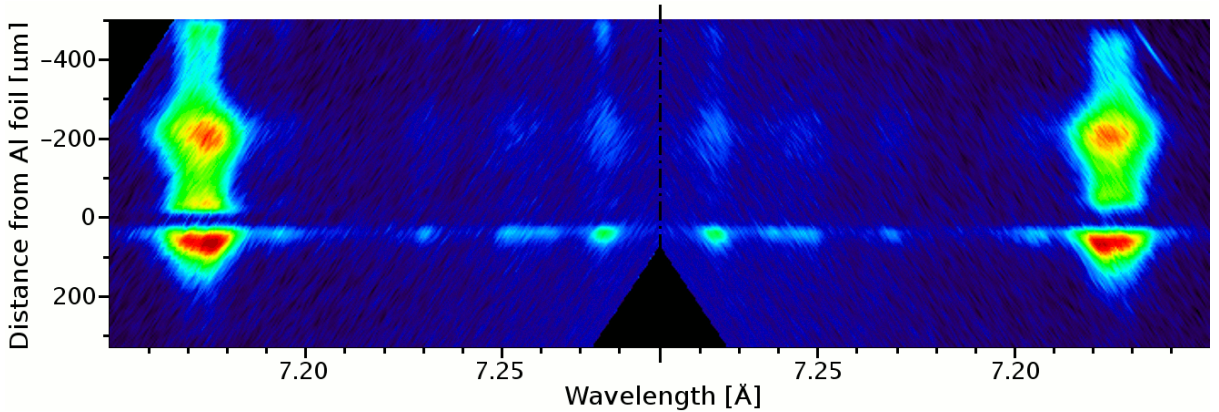


Figure 5.2: Spatially resolved spectra of the 2009 experiment.

The spectra shown in Fig. 5.2 (2009 experiment) correspond to the altered experimental configuration. The striking differences include:

- The gap in the line emission close to the position of the Al foil. This is explained by a small tilt of this foil, which partly blocks the radiation. (The laser beam was focused at the distance of approximately 200 - 500 μm from the foil edge.)
- The spectral lines display distinct second maximum in between the foils (at $\sim 200 \mu\text{m}$), while close to the second foil they do not reappear so significantly.

The strong emission at the midplane of the foils is again explained by a collision of two counter-streaming plasma jets. The plasma jet from the second foil was produced by the

5 Trial experiment evaluation

laser beam that burned through the first foil.

The observed difference corresponds to the diverse experimental conditions, in particular to the significant difference in laser frequency, which alters substantially the mechanism of energy deposition in the foils.

To summarize, in the first experiment the plasma jet collision with relatively cold Mg foil was observed, while in the second one we had observed the collision of two plasma jets. The more detailed interpretation of both experiments is a subject of further work.

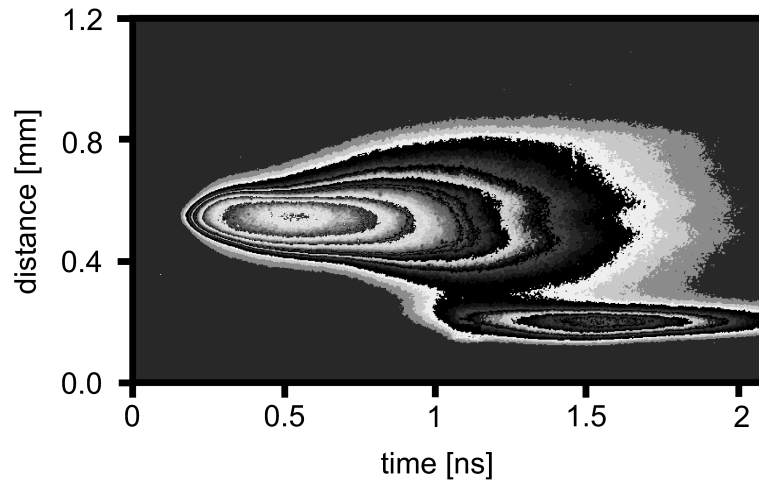


Figure 5.3: Spatially and temporally resolved emission from the streak camera of the 2006 experiment.

6 Conclusion

This thesis summarizes very briefly the problematics of plasma-wall interaction and demonstrates the possibility of its studies through the double-foil laser-plasma wall interaction experiments. The basic properties of instruments used in relevant experiments are presented, and the first results obtained by the novel codes for reconstruction of the measured spectra are shown.

I should emphasize that the measured high-resolution spectra can provide much more information on plasma interaction than the preliminary results discussed in this thesis. In particular, there is a substantial information potential in the satellite lines widths and positions depending on the spatial range of their emission. Further analysis of this data will be a subject of future investigation.

My personal contribution to this topic can be summarized in two points:

- Participation in experiments performed in January 2009.
- Design of the alternative approach to the VJS spectra processing. That consists of the spectra digitizing including the scanner calibration, and of design, testing and application of the novel *VJS Analyser* software package for spectra reconstruction, including its manual for its easy use (appendix A).

A VJS Analyser manual

A.1 Introduction

VJS Analyser is an application which analyzes raw x-ray data recorded by VJS spectrometer, as described in [3]. It is written in the Java language, so it needs a working Java Runtime Environment (JRE) to run. It was developed in 2009 by Michal Šmíd as a part of his bachelor thesis.

The basic functionality of this application consists in manipulating and analyzing the recorded spectral data from VJS spectrometer (which should be 16-bit gray-scale TIFF images) and exporting the resulting spectra into formats suitable for presenting and further analysis.

In this manual as well as in the application we use the unit Ångström ($1\text{Å} = 10^{-10}\text{m}$) for wavelengths, because it is often used in literature.

The contents of the software package is listed in table A.1.

File	Description
VJSA.JAR	Application main file, executable through JRE.
VJSA-RUN-LINUX.JAR	Launching script for Linux (see Section A.1.1)
VJSA-RUN-WINDOWS.BAT	Launching script for Windows (see Section A.1.1)
VJSA.CONF	Configuration file(see Section A.5)
VJSA MANUAL.PDF	This manual file.
LIB subdirectory	Directory containing necessary libraries.

Table A.1: Table of VJS Analyser package files.

A.1.1 Launching the application

The application is executable through the JRE. On some machines it may be possible to launch it by double-click the VJSA.JAR file, but this way is not recommended because the JRE will not allocate enough memory for the application.

The recommended way to launch the application is to type

```
java -Xmx512m -jar vjsa.jar
```

to the command line, which allocates 512 MB of memory for the application. Instead of typing this to the command line it is possible to run the VJSA-RUN-WINDOWS.BAT on Windows machines or VJSA-RUN-LINUX on Linux machines. Both scripts only perform the command written above.

A.1.2 Introduction to spectra reconstruction

Schematic view of the spectra production using VJS and definitions of axis and individual variables is shown in Fig. A.1.

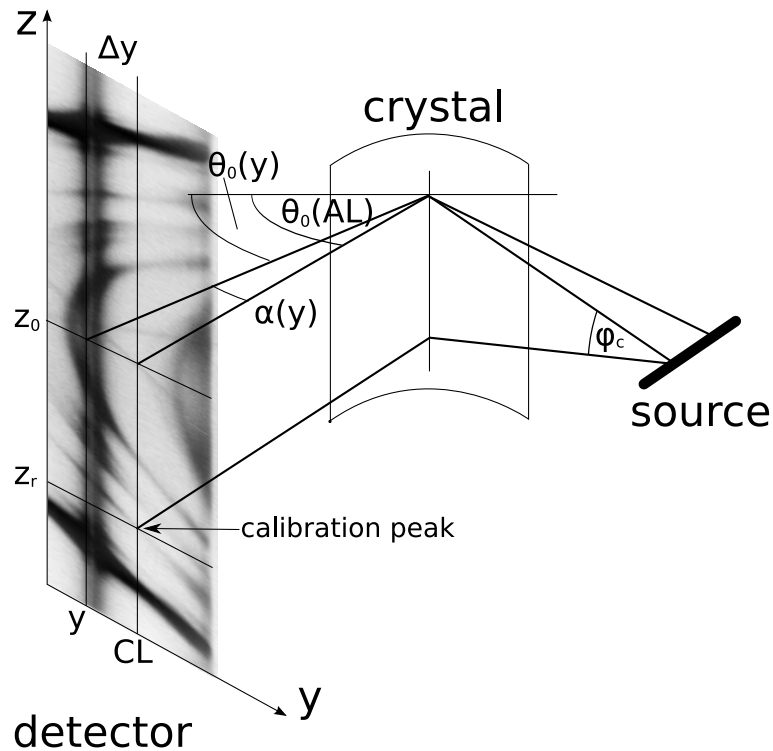


Figure A.1: Simplified scheme of VJS.

Hereafter we use these symbols:

- CL, ZL calibration and zero lines
- $2d$ 2d crystal interplanar spacing parameter
- l Source to crystal to detector distance
- λ_c Calibration peak's wavelength
- z_l, z_r Calibration peak's left and right z-positions

Use of terms horizontal and vertical is obvious from Fig. A.1 .

A.2 Image manipulation

VJS Analyser can handle basic image manipulation procedures. However, for advanced operations we recommend to use another graphic software (eg.: ImageJ ¹).

If there is any problem with image viewing, try choosing OTHER—REFRESH

A.2.1 Viewing an image

First, load desired image by choosing the IMAGE—LOAD command. The image is drawn in the right pane and the VIEW pane is shown. The viewing properties in this pane affect only the way the image is displayed on the screen. Those properties include:

- LIGHTNESS slider: increases the lightness of dark images. The leftmost position means no change.
- 8-BIT ONLY: increases the lightness by amount of 256, suitable if image is 8-bit only instead of recommended 16-bit.
- FIT WIDTH: If checked, shrinks the image width to fit the screen, otherwise the image is shown in its actual size.

A.2.2 Crop and Flip

To crop an image, choose IMAGE—CROP, then click into the image area to the point which will be the new upper-left corner, then to the one that will be the lower-right corner. Finally select IMAGE—CROP again and the image will be cropped.

The FLIP (HORIZ.AX.) and FLIP (VERT.AX.) operations flip the image around the appropriate axis.

¹<http://rsb.info.nih.gov/ij/>

A.2.3 Auto rotate

This feature lets you precisely measure the image rotation using the correlation algorithm, and consequently rotate it. It is based on the fact that the raw spectral data image is symmetrical with regard to the vertical axis and two symmetrically located small areas which are almost identical can be localized.

The algorithm searches the exact alignment of the left and right areas. This algorithm works fine only for images whose initial rotation is small (less than approximately 1°).

To use the auto rotation, follow these steps:

1. Select the IMAGE—AUTO ROTATE command.
2. In the image, select the left of the two significant, symmetrically placed, areas. This area is shown in the bottom pane.
3. Select the right of those two areas. It is shown in the bottom pane next to the first one. If necessary, you can now proceed to point 2 again to correct your selections.
4. Select the IMAGE—AUTO ROTATE command and the correlation is being processed. (It may take a while.) Its result is shown next to the areas with marked best correlation point. In the left area the best fitting point of the right one is also marked. In the ANGLE text field, the resulting angle is printed (in radians).
5. Now, you can either press the ROTATE button to process the rotation of the image given by the angle written in the ANGLE text field, or just use the measured value for realignment of the exposed film in film holder and scan it again.

A.3 Analyzing procedure

Before the analysis procedure can be performed, those conditions need to be fulfilled:

1. The raw data need to be properly loaded 16-bit gray-scale image.
2. The raw data need to be precisely rotated into horizontal position.
3. The arch-like shape of the spectral lines must “point to the bottom” as seen on Fig. A.2.
4. The image needs to be cropped so that there are no borders of the film left.

The analysis can be started by selecting the IMAGE—ANALYSE command. The ANALYSE pane will appear.

The numeric parameters should be set from the configuration file (see section A.5), but can be updated here. The horizontal lines are to be set here. Their setting is done



Figure A.2: Raw spectral data as should be loaded in VJS Analyser, with the horizontal lines marked on the right.

using horizontal cursor (green line inside the image). This cursor can be moved using the UP/DOWN arrows, the PAGE UP/PAGE DOWN keys or the mouse. After the cursor is in desired position, press the appropriate button and the line number is written next to the button.

Those horizontal lines are:

1. TOP LINE - Above this line no spectra will be analysed.
2. BOTTOM LINE - Below this line no spectra will be analysed.
3. ZERO LINE - This line defines the origin of spatial coordinate. (The surface/zero scan.)
4. CALIBRATION LINE - The line where the calibration peaks will be searched at.

Positions of those lines are shown in sample raw data image in figure Fig. A.2.

In the BOTTOM PANE, the calibration lineout is drawn. The number of points of this lineout is given by the ANALYZINGWAVERANGE parameter. The value of this parameter should be set sufficiently large to distinguish well the details of the profile analyzed.

To select the calibration peaks press the SET LEFT or SET RIGHT button and click into the lineout in the bottom pane approximately at the peak position. The given mouse horizontal position will be used as an initial parameter for the fit of the line profile function into the spectra. The result of this fit is drawn with red color into the plot and its wavelength is written next to the appropriate button. If there is no line drawn into the image, it means that the fit did not converge.

Finally, press the PROCESS button and the analysis will be performed. The DATA EXPORT pane will be shown.

A.3.1 Details of spectra line fit

The spectral lines are fitted using the least square algorithm. The fitting function f is the Gaussian profile modified to correspond the profile deformation given by the spectrometer geometry,

$$f(z) = G(\lambda(z)), \quad (\text{A.1})$$

where $G(x)$ is the Gaussian profile

$$G(x) = ae^{-\frac{(x-x_0)^2}{2\sigma^2}} + b, \quad (\text{A.2})$$

and $\lambda(z)$ is the function converting the z coordinate defined in Fig. A.1 into the wavelength,

$$\lambda(z) = \lambda_0 \cos\left(\text{atan}\left(\frac{z}{l}\right)\right) \quad (\text{A.3})$$

where l is the source to crystal to detector distance and λ_0 is the maximal wavelength in the current raw spectra lineout.

During the fit, the parameters a, b, x_0 and σ are being fitted, while l and λ_0 are fixed. (l is the DISTANCE analyzing parameter, and λ_0 is computed from the analyzing parameters.)

This complicated function is necessary, because the wavelength axis of the lineout is not linear and therefore the line profiles in the lineout are not symmetrical.

A.3.2 Details of spectra reconstruction

Here we describe the crucial routine of this application, the spectra reconstruction, which transforms the raw spectral data in the scanned image into a set of spectra.

A.3.2.1 Preparation

1. Each pixel of the image is converted into the light intensity using formulae (A.6) and (A.9). (see sections A.5.3 and A.5.4)
2. $z_0 = \frac{z_l + z_r}{2}$ is the vertical central position in the raw data.
3. $\varphi_c = \text{atan}\left(\frac{z_r - z_0}{l}\right)$ is the vertical divergence angle of the ray defined by the source and the calibration peak positions.
4. $\theta_0(CL) = \text{asin}\left(\frac{\lambda_c}{2d \cos(\varphi_c)}\right)$ is the Bragg angle (the glancing angle of incidence on the crystal) of the central ray defined by the symmetry axis of the calibration lineout.

A.3.2.2 Transformation

For each spectral lineout within the top and bottom lines (corresponding to a given y), the following is performed:

1. $\Delta_y = (CL - y)$ is the horizontal distance from the calibration line.
2. $\alpha(y) = \text{atan}(\frac{2}{l} \Delta_y)$ is the horizontal divergence angle of the ray going from the crystal to the detector.
3. $\theta_0(y) = \theta_0(CL) + \alpha(y)$ is the Bragg angle of the central ray in the lineout defined by the y coordinate.
4. $\lambda_0(y) = 2d \sin(\theta_0(y))$ is the wavelength corresponding to the spectrum symmetry axis in the y line.

The wavelength range covered in the spectrum studied is split into a set of equidistant intervals. The width of each interval is given by the EXPORTWAVELENGTHSTEP parameter. The z -coordinates of the interval boundaries are computed using equation

$$z = z_0 \pm l \tan(\text{acos}(\frac{\lambda}{\lambda_0(y)})), \quad (\text{A.4})$$

where the \pm sign differs the left and the right hand spectra. Note that while on the wavelength scale the intervals are equidistant, in z coordinates they are not. Generally, there are more data points in the same wavelength interval positioned close to the spectra symmetry axis, i.e. at the longer wavelengths.

A.4 Data export

After the analysis is performed, the DATA EXPORT pane is shown and the reconstructed spectra is drawn in the right pane.

In this phase you can examine the spatially resolved spectra, and export them into tables and easily readable images.

All types of export use the current values of the parameters MINIMAL and MAXIMAL WAVELENGTH, and WAVELENGTH STEP, as set in the text fields in the left pane.

With respect to these parameters, only the interval given by the MINIMAL and MAXIMAL WAVELENGTH is exported, and the interval between each two neighboring exported pixels/points is given by the WAVELENGTH STEP parameter. The total number of exported pixels/points is then computed as

$$\text{number of points} = \frac{\lambda_{max} - \lambda_{min}}{s} + 1, \quad (\text{A.5})$$

where λ_{max} , λ_{min} , and s are the parameters MINIMAL and MAXIMAL WAVELENGTH, and WAVELENGTH STEP.

The EXPORT DIRECTORY, into which the tables and plain images are exported, can be set using the CHANGE button.

A.4.1 Export as tables

Exports the spectrum under current cursor position as two separated files, LXXX.DAT and RXXX.DAT for the left and the right hand part of the evaluated spectrum, respectively, where XXX denotes the spatial position of the spectrum written in 3 digits in μm . The files are saved into the EXPORT DIRECTORY.

The tables are simple text files, where each row corresponds to one point in the spectral plot and has a format WAVELENGTH <TAB> INTENSITY.

A.4.2 Export as plain image

Exports data into the file PLAINIMAGE.TIF, which is a 2D plot, with the X-axis corresponding to the wavelength [\AA] and the Y-axis to the position [μm]. Each pixel value represents a radiation intensity with corresponding wavelength and position. The information about the scale and the calibration of the image is in the PLAINIMAGEINFO.TXT.

Both files are saved into the current EXPORT DIRECTORY.

A.4.3 Export as labeled image

Exports a 2D image similar to the *plain image*, but optimized for presenting. After the button is pressed, the save dialog appears to ask for the desired filename of the image, i.e. disregarding the export directory.

The new features of the labeled image include:

- Intensity mapping to colors. (Using internally built colormap.)
- Labels on edges of the image. (with tick and text intervals defined using the IMAGE...INT parameters)
- The image quality enhancement using the INTELIBLUR option (which is applied if the checkbox is checked). This option performs a kind of selective blur, which is optimized for the noise that can be present in the image.

A.4.4 Examining spectra

The horizontal cursor can be moved similarly as in the previous phase, using the UP/DOWN arrows, PAGE UP/PAGE DOWN keys or the mouse. The actual spectral record is shown in the bottom pane and its spatial position (distance from the zero line) denoted as y is written in the left pane (in μm).

To examine the spectra, you can click into the lineout in the bottom pane and the wavelength corresponding to the mouse position and the intensity in this position is written in the left pane. The intensity is in the same units as those given in the calibration formula (A.9).

A.5 Configuration

This application is configured through the configuration file, which sets the values of several parameters. Because most of them are specific for each experiment, we recommend to have one configuration file for each experiment setup and just copy the appropriate file in the application directory. The file is loaded when launching the application. If the configuration is changed during the application run, the modified configuration file can be reloaded using the OTHER—RELOAD CONFIGURATION command.

A.5.1 Table of parameters

Table A.2 sums up all application parameters, their default or recommended values, their description, and a reference to a section in this manual. The parameters written in bold letters can be set during the analysis process (their values stated in the configuration file are considered as default values only), the others must be defined in the configuration file.

A.5.2 Configuration file syntax

The calibration file named VJSA.CONF is located in the same directory as the program VJSA.JAR file. It is a plain text file. Each row represents one parameter assignment. All rows beginning with the number sign (#) and empty rows are ignored. All values are float, except pixel unit values, which are integers. A preview of calibration file can be seen in Fig. A.3.

Parameter	Value	Description	Sec.
Experimental setup			
2d	8.5084 [Å]	VJS crystal interplanar spacing parameter (2d).	
Distance	104.718 [mm]	Source to crystal to detector distance.	
PeakWavelength	7.2759 [Å]	Wavelength of the spectral line used for calibration.	
ScanResolutionSpatial	4800 [dpi]	Scanned raw data tiff file spatial resolution.	
ScanResolutionWavelength	4800 [dpi]	Scanned raw data tiff file wavelength resolution.	
Export parameters			
exportWavelengthStep	0.0001 [Å]	Wavelength step between points exported.	A.4
exportMinWavelength	7.15 [Å]	Minimal wavelength contained in the exported data.	A.4
exportMaxWavelength	7.30 [Å]	Maximal wavelength contained in the exported data.	A.4
imageWavelengthTextInt	0.05 [Å]	Interval between wavelength labels.	A.4.3
imageWavelengthTickInt	0.05 [Å]	Interval between wavelength ticks.	A.4.3
imagePositionTextInt	200 [μm]	Interval between position labels.	A.4.3
imagePositionTickInt	100 [μm]	Interval between position ticks.	A.4.3
Internal parameters, calibration			
AnalyzingWaveRange	750 [px]	Number of points of spectra used during calibration peak recognition.	A.3
oda..odd		constants of scanner calibration	A.5.3
precalibrated	0 [0/1]	set to 1 if raw data are calibrated	A.5.3
a0..a3		constants of film calibration	A.5.4
BackgroundValue	41300	Scanned tiff value of the developed, unexposed film	A.5.4

Table A.2: List of application parameters.

A VJS Analyser manual

```
#VJS Analyser configuration file
#for documentation see included manual.pdf file

### scanner calibration
precalibrated = 0
oda = 0.7727
odb = 0.00121771
odc = -1.56752
odd = 3.12334

### film calibration (depending on film , and photon energy)
#(the film calibration section need to be below
# the scanner calibration section)
a0 = -0.08002
a1 = 1.48876
a2 = -0.10975
a3 = 0.18192
backgroundvalue = 41300

### Experimental setup
2d = 8.5084
Distance = 104.718
PeakWavelength = 7.2759
ScanResolutionSpatial = 4800
ScanResolutionWavelength = 4800

### Export parameters
exportWavelengthStep = 0.0001
exportMinWavelength = 7.15
exportMaxWavelength = 7.30

imageWavelengthTextInt = 0.05
imageWavelengthTickInt = 0.05
imagePositionTextInt = 200
imagePositionTickInt = 100

### Internal parameters
AnalyzingWaveRange = 750
```

Figure A.3: Preview of sample calibration file VJSA.CONF.

A.5.3 Scanner calibration

The relation between the measured optical density (D_m) of the scanned material and a pixel value in a scanned tiff file (v) is generally given by

$$D_m = -a \log_{10}(bv + c) + d, \quad (\text{A.6})$$

where the constants $a \dots d$ need to be measured for the current scanner and set into the configuration file where they are listed as ODA. . . ODD.

A.5.3.1 precalibrated data

The application can also handle data from devices which are already calibrated to the optical densities. In this case, it is necessary to switch the PRECALIBRATED option to true. That means that in the configuration file should be line containing

```
precalibrated = 1
```

and the optical density of the film (D_f) is get from the equation

$$D_f = a + bv, \quad (\text{A.7})$$

where a and b are the calibration constants ODA and ODB and v is the scanned tiff file value. Note that in this regime, the film base subtraction (equation A.8) is not performed.

A.5.4 Film calibration

The film calibration relates the recalculation of the photon fluxes impinging on the film (I [ph/ μm^2]) to the measured optical density (D_m).

First we need to determine the optical density of the sensitive layer of the film (D_f) only. That is done by subtracting the optical density of the developed, unexposed film (D_b),

$$D_f = D_m - D_b. \quad (\text{A.8})$$

We can simply subtract this values because of the additivity of the optical density. The D_b is calculated from the parameter BACKGROUNDVALUE using (A.6). The BACKGROUNDVALUE should be measured in the scanned file of the developed, unexposed film.

Second, we apply the relation between D_f and the intensity, the so called characteristic curve of the given x-ray film.

A VJS Analyser manual

This relation depends on the energy of the measured photons; within the small range of energies covered at the given VJS setup, this dependence is negligible. For each photon the characteristic curve can be described by the third degree polynomial (expressed in units of $\text{ph}/\mu\text{m}^2$) :

$$I = a_0 + a_1 D_f + a_2 D_f^2 + a_3 D_f^3, \quad (\text{A.9})$$

where the values $a_0 \dots a_3$ are known from the independent film calibration and need to be set in the calibration file as the parameters A0 ... A3.

Bibliography

- [1] D. Salzmann. *Atomic Physics in Hot Plasmas*. Oxford University Press, 1998.
- [2] A. Cejnarova, L. Juha, B.Kralikova, J. Krasa, E.Krousky, P.Krupickova, L.Laska, K.Masek, T.Mocek, M.Pfeifer, A. Präg, O.Renner, K.Rohlana, B.Rus, J.Skala, P.Straka, J.Ullschmied, and K. Jungwirth. The Prague Asterix laser system. *Phys. Plasmas*, 8:2495, 2001.
- [3] O. Renner, T. Missalla, P. Sondhauss, E. Krouský, E. Förster, C. Chenais-Popovics, and O. Rancu. High-luminosity, high-resolution, x-ray spectroscopy of laser-produced plasma by vertical-geometry johann spectrometer. *Rev. Sci. Instrum.*, 68 (6):2393, June 1999.
- [4] O. Renner. *Pokročilá rentgenová spektroskopie vysokoteplotního hustého plazmatu*. PhD thesis, Institute of Physics, AS CR, 1998.
- [5] O.Renner, F.B.Rosmej, P.Adámek, E.Dalimier, A.Delserieys, E. Krouský, J.Limpouch, R.Liska, D.Riley, and R.Schott. Spectroscopic characterization of ion collisions and trapping at laser-irradiated double-foil targets. *High Energy Density Physics*, 3:211, 2007.